HHS Public Access

Author manuscript

Ophthalmology. Author manuscript; available in PMC 2018 May 01.

Published in final edited form as:

Ophthalmology. 2017 May ; 124(5): 709–719. doi:10.1016/j.ophtha.2017.01.004.

Peripapillary and Macular Vessel Density in Glaucoma Patients with Single-Hemifield Visual Field Defect

Adeleh Yarmohammadi, MD[1], **Linda M. Zangwill, PhD**[1], **Alberto Diniz-Filho, MD, PhD**[1], **Luke J. Saunders, PhD**[1], **Min Hee Suh, MD**[1,2], **Zhichao Wu, BAppSc(Optom), PhD**[1], **Patricia Isabel C. Manalastas, MD**[1], **Tadamichi Akagi, MD, phD**[1,3], **Felipe A. Medeiros, MD, PhD**[1], and **Robert N. Weinreb, MD**[1]

[1]Hamilton Glaucoma Center, Shiley Eye Institute, Department of Ophthalmology, University of California San Diego, La Jolla, CA

[2]Haeundae Paik Hospital, Inje University, Busan, South Korea

[3]Department of Ophthalmology and Visual Sciences, Kyoto University Graduate School of Medicine, Kyoto, Japan

Abstract

Purpose—To compare hemifield differences in the vessel density of the optic nerve head and macula in open-angle glaucoma (OAG) eyes with visual field (VF) defect confined to one hemifield using optical coherence tomography angiography (OCT-A).

Design—Cross-sectional study.

Participants—Fifty-eight eyes of 58 glaucoma patients with VF loss confined to a single hemifield, and 28 healthy eyes.

Methods—Retinal vasculature information was summarized as circumpapillary vessel density (cpVD) and perifoveal vessel density (pfVD). Circumpapillary retinal nerve fiber layer (cpRNFL) and macular ganglion cell complex (mGCC) thickness were also calculated using spectral domain OCT. Paired and unpaired t-tests were utilized to evaluate differences between the perimetrically affected and intact hemiretinae and healthy hemiretinae. Linear regression analyses were performed to evaluate the associations between VF measures with vascular and structural measurements.

Correspondence: Robert N. Weinreb, MD, Hamilton Glaucoma Center, Department of Ophthalmology, University of California, San Diego, 9500 Gilman Drive, La Jolla, CA, 92093-0946, rweinreb@ucsd.edu.

Financial Disclosure(s): Adeleh Yarmohammadi: none; Linda M. Zangwill: Research support – Carl Zeiss Meditec, Heidelberg Engineering, National Eye Institute, Topcon, and Nidek; Alberto Diniz-Filho: none; Luke J. Saunders: none; Min Hee Suh: none; Zhichao Wu: none; Patricia Isabel Manalastas: none; Tadamichi Akagi: none; Felipe A. Medeiros: Financial support – Alcon, Allergan, Bausch & Lomb, Carl Zeiss Meditec, Heidelberg Engineering, Merck, Reichert, Sensimed, and Topcon; Research support – Alcon, Allergan, Carl Zeiss Meditec, National Eye Institute; and Reichert; Consultant – Allergan, Carl Zeiss Meditec, and Novartis; Robert N. Weinreb: Research support –Carl Zeiss Meditec, Genentech, Heidelberg Engineering, National Eye Institute, Optovue, and Topcon; Consultant – Alcon, Allergan, Bausch & Lomb, Forsight V, Unity.

Main Outcome Measures—Total and hemispheric cpVD, pfVD, cpRNFL, mGCC and mean sensitivity (MS).

Results—Mean cpVD and pfVD in the intact hemiretinae of OAG eyes (59.0% and 51.1%) were higher than the affected hemiretinae (54.7% and 48.3%; p<0.001) but lower than healthy eyes (62.4% and 53.8%; p<0.001). Similar results were noted with cpRNFL and mGCC thickness measurements (p<0.05 for both). The strongest associations between MS in the affected hemifields were found for cpVD (r = 0.707), followed by pfVD (r = 0.615), cpRNFL (r = 0.496) and mGCC (r = 0.482) in the corresponding hemiretinae (p<0.001 for all). Moreover the correlations in the intact hemifields between MS with cpVD and pfVD were found to be higher (r = 0.450 and 0.403) than the correlations between MS and cpRNFL and mGCC thickness measurements (r = 0.340 and 0.290; all p-values <0.05 for all).

Conclusions—Reduced peripapillary and macular vessel density was detectable in the perimetrically intact hemiretinae of glaucoma eyes with a single-hemifield defect. Moreover vessel density attenuation in both affected and intact hemiretinae was associated with the extent of VF damage in the corresponding hemifields. OCT-A potentially shows promise for identifying glaucomatous damage before focal VF defects are detectable.

Introduction

Glaucoma is a multifactorial optic neuropathy of unknown etiology.[1] There is mounting evidence that vascular factors play a role in the pathogenesis of the disease.[2, 3] However the study of ocular vasculature in glaucoma has been a challenge due to several limitations in the imaging modalities;[4-7] therefore the contribution of ocular vasculature in the pathogenesis of glaucoma has remained unclear. Several studies have shown that structural injury often precedes detectable visual field loss as measured by standard automated perimetry (SAP).[8-11] In eyes with visual field damage confined to a single-hemifield, there is evidence that both the retinal nerve fiber layer (RNFL) and the macular ganglion cell complex (mGCC) thickness are reduced even in the retinal hemispheres corresponding to the perimetrically intact hemifields.[12-14] However, there is limited information on whether the microvasculature is reduced in eyes with localized glaucomatous functional loss, and its possible contribution to the natural course of the disease.[15]

Optical coherence tomography angiography (OCT-A)[16] is a non-invasive imaging technique that provides reproducible quantitative assessment of the vasculature in the optic nerve, peripapillary retina and macula.[17-20] Recent reports using OCT-A in glaucoma eyes documented attenuation of vasculature in the optic nerve head [17, 19] and peripapillary area.[18, 19, 21] However, there is limited evidence about the extent of microvascular damage in eyes with more localized glaucomatous defects [22, 23] and, to our knowledge, there are no reports characterizing vasculature in the macula of eyes with glaucoma.

The objective of the present study was to quantitatively assess the retinal vessel density of the peripapillary and macula in the perimetrically intact hemiretinae of glaucoma eyes with single-hemifield focal visual field defects using OCT-A. A further aim was to evaluate the associations between vessel density measures in both affected and intact hemiretinae with the extent of visual field damage in their corresponding hemifields.

Methods

Study Participants

A total of 58 glaucoma patients and 28 healthy controls meeting the eligibility criteria were recruited from the longitudinal Diagnostic Innovations in Glaucoma Study (DIGS) conducted at the Hamilton Glaucoma Center, University of California, San Diego (UCSD). The DIGS protocol and eligibility criteria have been previously described.[24] Informed consent was obtained from all participants. The University of California San Diego Institutional Review Board approved all protocols and methods described adhered to the tenets of the Declaration of Helsinki and the Health Insurance Portability and Accountability Act (HIPAA).

As part of the DIGS protocol all study participants underwent a complete ophthalmologic examination, including assessment of best-corrected visual acuity (BCVA), slit-lamp biomicroscopy, IOP measurement with Goldmann applanation tonometry, gonioscopy, ultrasound pachymetry, dilated fundus examination and simultaneous stereophotography of the optic disc. Systemic measurements included two blood pressure (BP) measurements obtained using an Omron Automatic (Model BP791IT, Omron Healthcare, Inc., IL, USA) blood pressure instrument. Mean arterial pressure was calculated as 1/3 systolic BP + 2/3 diastolic BP. Mean ocular perfusion pressure (MOPP) was defined as the difference between 2/3 of mean arterial pressure and IOP.

Participants also completed OCT-A (Angiovue; Optovue, Inc., Fremont, CA, USA) and SD-OCT (Avanti; Optovue, Inc.) optic nerve head imaging along with standard automated perimetry (SAP). Inclusion criteria common to DIGS participants were age of over 18 years, open angles on gonioscopy, and BCVA of 20/40 or better. Participants included in this study were required to have good quality OCT-A and SD-OCT imaging and also have ≥ two reliable SAP tests. Further inclusion criteria for glaucoma patients were: 1) Repeatable glaucomatous visual field damage defined as a Glaucoma Hemifield Test (GHT) result outside normal limits and a Pattern Standard Deviation (PSD) outside 95% normal limits and 2) Glaucomatous visual field abnormalities exclusively in one hemifield as defined by a cluster of ≥ 3 adjacent points in the pattern deviation (PD) plot with a probability of less than 5% including at least one point having a probability less than 1% in at least two repeatable and consecutive SAP tests. A perimetrically intact hemifield required having no test points with a probability level less than 2% or no clusters of ≥ 3 adjacent points with a probability of less than 5% on the PD plot. Eyes that were included in the present study had visual field abnormalities such as focal scotomas, nasal steps, arcuate scotomas, altitudinal defects, or any other abnormalities that met our inclusion criteria. If both eyes met the inclusion criteria, one eye was randomly selected for analysis. Healthy controls were required to have: 1) an intraocular pressure (IOP) <21 mmHg with no history of elevated IOP, 2) normal appearing optic disc, intact neuroretinal rim and RNFL on clinical examination, and 3) a minimum of two reliable normal visual fields, defined as a PSD within 95% confidence limits and a GHT result within normal limits.

Exclusion criteria common to both study groups were history of intraocular surgery (except for uncomplicated cataract surgery or glaucoma surgery), coexisting retinal pathologies,

non-glaucomatous optic neuropathy, uveitis, or ocular trauma. Participants with systemic hypertension and diabetes mellitus were included unless they were diagnosed with diabetic or hypertensive retinopathy. Participants with unreliable visual field results, poor quality OCT-A, or SD-OCT scans were also excluded from this study.

Standard Automated Perimetry

Standard automated perimetry visual field tests were performed using Swedish Interactive Threshold Algorithm (SITA) standard 24-2 threshold test (Humphrey Field Analyzer 750 II-I, Carl Zeiss Meditec, Inc., Dublin, CA, USA). All participants that were included were familiar with SAP testing from earlier exposure to at least two visual field examinations.

The quality of visual field tests was reviewed by the Visual Field Assessment Center (VisFACT) staff at UCSD. Only participants with reliable tests (≤ 33% fixation losses and false negative errors, and ≤ 15% false positive errors) were included in this study. Visual fields that were found to have the following artifacts were also excluded: evidence of rim and eyelid artifacts, inattention or fatigue effects, or visual field damage caused by a disease other than glaucoma.

For hemifield specific analyses in the glaucoma eyes, the average total deviation (TD), pattern deviation (PD) and mean sensitivity (MS) were calculated in each hemifield based on the individual test points excluding the blind spot. Sensitivity in dB at each test location was also converted to the linear scale of 1/Lambert (1/L) and then averaged to obtain MS values in a linear scale in each hemifield. In the healthy eyes, the “intact” hemifield was randomly selected and visual field indices were calculated in a similar fashion.

OCT Angiography Image Acquisition and Processing

All subjects underwent OCT-A imaging with a commercially available OCT-A system, the Angiovue (Optovue, Inc.) that is incorporated in the Avanti SD-OCT system. The Angiovue imaging system provides a non-invasive method of characterizing the vascular structures of the retina at the capillary level. Details of this technology have been described elsewhere.[25] Briefly, it uses the Split-Spectrum Amplitude-Decorrelation Angiography (SSADA) algorithm to capture the dynamic motion of moving particles such as red blood cells and provides a high-resolution 3D angiogram of perfused retinal vasculature (Figure 1). The Angiovue characterizes vascular information at various user-defined retinal layers [26] qualitatively as a vessel density map and color-coded vessel area density (Figure 3). Quantitatively it provides vessel density (%) measurements calculated as the percentage of measured area occupied by flowing blood vessels being defined as pixels having SSADA algorithm based decorrelation values above the threshold level.

For the present study, peripapillary vessel density was derived from the images acquired with a 4.5×4.5 mm field of view centered on the optic disc. Macular vessel density measurements were calculated from 3×3 mm scans centered on the fovea. For both measurement regions segmentation was performed using the OCT intensity B-scans. Peripapillary vessel density measurements were calculated within the RNFL in a slab from the internal limiting membrane (ILM) to the RNFL posterior boundary. Macular superficial

vessel density measurements were calculated in a slab from ILM to the posterior boundary of the inner plexiform layer (IPL).

Total and hemispheric measurements of the vasculature were obtained in two regions: 1) Total circumpapillary vessel density (cpVD) was calculated in a region defined as a 750-μm-wide elliptical annulus extending from the optic disc boundary based on 360 degree global area and eight 45 degree sectors as shown in figure 1 and 3. Hemispheric measurements were calculated by averaging the four sectors in each hemiretinae: superior hemispheric measurements were calculated by averaging the measurements in the supero-temporal (ST), temporal-upper (TU), supero-nasal (SN) and nasal-upper (NU) and inferior hemispheric measurements were derived from average measurements in the infero-temporal (IT), temporal-lower (TL), infero-nasal (IN) and nasal-lower (NL). 2) Total perifoveal vessel density (pfVD) was measured in an annular region with an inner diameter of 1 mm and outer diameter of 2.5 mm centered on the fovea; The perifoveal region was divided into the superior and inferior hemiretinal areas to calculate the hemispheric measurements in each hemiretinae as shown in Figure 1 and 3.

Trained graders reviewed the quality of all OCT-A scans using a standard protocol established by the Imaging Data Evaluation and Analysis (IDEA) reading center at UCSD. Poor quality scans were excluded from the analysis if one of the following criteria were met: 1) signal strength index (SSI) of lower than 48 (1= minimum, 100 = maximum), 2) poor clarity images, 3) local weak signal caused by artifacts such as floaters, 4) residual motion artifacts visible as irregular vessel patterns or disc boundary on the enface angiogram and 5) RNFL segmentation failure.

Spectral Domain OCT Imaging

Optic nerve head and macular imaging were also performed using the Avanti SD-OCT system on the same day as OCT-A imaging and by the same operator. Avanti SD-OCT uses a light source with center wavelength of 840 nm and it has an A –scan rate of 70-kHz. The ONH scanning protocol was used for measuring the cpRNFL thickness and the macular ganglion cell (mGCC) scanning protocol was utilized to measure the mGCC thickness.

Specifically, the ONH map protocol calculates circumpapillary RNFL (cpRNFL) thicknesses in a 10 pixel-wide band along a circle of 3.45 mm in diameter centered on the ONH based on 360-degree global area and eight 45-degree sectors. Global average and hemispheric measurements corresponding to the superior and inferior hemifields were used for the analysis in the present study. Hemispheric measurements were calculated by averaging the four circumpapillary RNFL sectors (ST, TU, SN, NU in the superior hemiretinae) and (IT, TL, IN, NL in the inferior hemiretinae) as shown in Figure 1.

The mGCC scanning protocol consists of a 7×7 mm^2 raster scan consisting of 1 horizontal B scan of 933 A-scans, 15 vertical B scans of 933 A-scans per B-scan. This protocol measures retinal thickness from the ILM to the IPL posterior boundary obtained from the raster scans and mGCC thickness measurements consist of the ganglion cell layer, IPL and RNFL. The mean mGCC thickness and also measurements in the superior and inferior hemispheres were used for the analysis. Only good-quality ONH and GCC images, defined by scans with SSI

≥ 37, and without segmentation failure or artifacts such as missing or blank areas were included for the analysis.

Statistical Analyses

The distribution of numerical variables was assessed by inspecting histograms and using Shapiro-Wilk W tests of normality. Numerical data were presented as the mean and standard deviation (SD). The independent two sample student *t*-test was used for group comparison of normally distributed variables; the Mann-Whitney U-test was used to assess for continuous non-normal variables and the Chi-square test was employed to compare categorical variables among groups.

Total and hemispheric OCT-A-derived vessel density measurements, SD-OCT-derived cpRNFL and mGCC thickness measurements, and visual field indices were compared between glaucoma and healthy eyes using the independent two sample *t*-test or the Mann–Whitney U-test. Two-tailed paired *t*-test and Wilcoxon signed-rank order tests were used to compare hemispheric measurements between perimetrically affected and intact hemiretinae in glaucoma eyes. Linear regression analyses and Pearson correlation coefficients (r values) were used to investigate the associations between structural and vascular measurements of the affected and intact hemiretinae and SAP parameters in the corresponding hemifields, including hemispheric MS, PD and TD.

Statistical analyses were performed using Stata version 14 (StataCorp, College Station, TX), and JMP version 11.2.0 (SAS Inc., Cary, NC). P values (type I error) of less than 0.05 were considered statistically significant for all analyses.

Results

Demographics and clinical characteristics of study subjects are summarized in Table 1. There were no significant differences in age, gender, refractive error, CCT and SD-OCT-derived disc area measurements between glaucoma and healthy eyes ($p > 0.05$ for all). Self-reported history of hypertension, diabetes mellitus, and cardiovascular diseases and also the prevalence of taking systemic antihypertensive and diabetic medications were also similar between the two groups ($p > 0.05$ for all). IOPs were higher in healthy eyes than treated glaucoma eyes. but this difference did not reach statistical significance ($p = 0.076$). Differences in SBP, DBP and MOPP between groups also did not reach statistical significance ($p > 0.05$).

As expected, glaucoma eyes had on average worse VF MD and VF PSD and thinner rim area, cpRNFL and mGCC values compared to healthy eyes ($p < 0.001$ for all). OCT-A global average peripapillary and macular vascular measurements were also significantly lower in glaucoma eyes (cpVD: 57.0 ± 4.7 % and pfVD: 49.7 ± 3.1 %) compared to healthy eyes (cpVD: 62.5 ± 3.6 % and pfVD: 53.9 ± 2.4 %; $p < 0.001$ for both comparisons).

In the glaucoma group, the glaucomatous visual field defect was localized to the superior hemifield in 26 of 58 eyes (44.8%) and to the inferior hemifield in 32 eyes (55.2%). Therefore 13 superior (46.4%) and 15 inferior (53.6%) hemifields and corresponding

hemiretinae of healthy eyes were randomly selected as control matched to the intact hemifields and hemiretinae of glaucoma eyes. In healthy eyes, visual field MS, PD and TD did not significantly differ between the two hemifields (paired t-test; $p > 0.05$ for all comparisons). In glaucoma eyes however, MS in the perimetrically intact hemifields (29.0 ± 1.8 dB; 854.1 ± 332.0 1/Lambert) was significantly higher than the MS values in the affected hemifields (26.0 ± 3.7 dB; 513.9 ± 349.6 1/Lambert; $p < 0.001$). Average visual field TD and PD values of the intact hemifields of glaucoma eyes (-0.1 ± 1.4 dB and -1.3 ± 0.3 dB respectively) were also significantly higher than the corresponding values in the affected hemifields (-6.7 ± 6.4 dB and -7.3 ± 6.1 dB respectively; $p < 0.001$). It is worth noting that these visual field measurements in the intact hemifields of glaucoma eyes were slightly lower than values in the hemiretinaes of healthy eyes but the differences did not reach statistical significance ($p > 0.05$, Table 2).

Qualitatively, capillary networks in both peripapillary and macular vascular regions of healthy eyes were denser compared to glaucoma eyes (Figure 3). In addition, the areas of reduced vessel density in the glaucoma eyes corresponded well with the location of visual field damage and RNFL and GCC thinning (Figure 1 and 2). Moreover, no differences were found between the peripapillary and macular vasculature in the superior and inferior hemiretinae of healthy eyes (Figure 3). In glaucoma eyes by contrast, more areas of reduced vessel density can be detected in the affected hemiretinae compared to the intact hemiretinae. Quantitatively, OCT-A cpVD and pfVD, and cpRNFL and mGCC thickness measurements in healthy eyes, did not significantly differ between two hemifields (paired t-test; $p > 0.05$ for all comparisons). In contrast, in glaucoma eyes OCT-A cpVD and pfVD, and cpRNFL and mGCC thickness measurements were significantly reduced in the affected hemiretinae compared to the perimetrically intact hemiretinae (Table 2). Specifically cpVD (54.7 ± 5.3 %), pfVD (48.3 ± 4.2%), cpRNFL (72.1 ± 10.9 μm) and mGCC thickness measurements (74.7 ±7.8 μm) in the affected hemiretinae were lower than cpVD (59.0 ±3.1 %), pfVD (51.1 ± 2.4 %), cpRNFL (83.6 ± 9.3 μm) and mGCC thickness (87.3 ± 5.8 μm) measurements in the intact hemiretinae ($p < 0.001$ for all comparisons).

The structural and vessel density measures in the intact hemiretinae of glaucoma eyes with similar measurements in healthy hemiretinae of control eyes were also compared. As illustrated in Figure 3, reduced vessel density was observed in the intact hemiretinae of glaucoma eyes compared with healthy eyes in both peripapillary and macular regions. Results of the quantitative analysis also showed that both vascular and structural measurements were lower in the intact hemiretinae of glaucoma eyes compared with healthy hemiretinae (Table 2).

The correlations between reduced vessel density, RNFL and GCC atrophy in both affected and intact hemiretinae with the severity of glaucomatous visual field loss in the corresponding hemifields are summarized in Table 3 and illustrated in Figures 4 and 5.

In the affected hemifields, the strongest associations between visual field MS with vascular and structural measurements in the corresponding hemiretinae were found for cpVD ($r = 0.707$), followed by pfVD ($r = 0.615$), cpRNFL ($r = 0.496$) and mGCC ($r = 0.482$; $p < 0.001$ for all) (Figure 4). In the perimetrically intact hemifields, the strongest associations were

found between visual field MS and cpVD (r = 0.450), followed by pfVD (r = 0.403), cpRNFL (r = 0.340) and mGCC (r =0.290; $p < 0.05$ for all) (Figure 5).

Discussion

In the present study, the OCT-A peripapillary and macular vascular measures as well as SD-OCT cpRNFL and mGCC thickness measurements were significantly reduced in the affected hemiretinae compared with perimetrically intact hemiretinae in glaucoma eyes with single-hemifield visual field defects ($p < 0.001$ for all comparisons). As expected in healthy eyes, vascular and structural measurements did not significantly differ between superior and inferior hemiretinae ($p > 0.05$ for all comparisons). Moreover, areas of reduced vessel density could be detected qualitatively and quantitatively even in the intact hemiretinae of glaucoma eyes compared to healthy eyes in both the peripapillary and macular regions ($p < 0.002$). These findings suggest that vascular changes may precede detectable visual field damage, and that hemodynamic deficiencies in addition to the structural damage might have already commenced in the peripapillary and macular regions of the apparently normal hemiretinae of glaucoma eyes with localized visual field damage. However the mechanism by which it occurs remains unclear.

Several studies have shown the presence of glaucomatous RNFL and GCC defects in the retinal hemispheres corresponding to intact hemifields of glaucoma eyes with single-hemifield visual field defects.[13-15] In agreement with our results, these studies showed that mean RNFL and GCC thickness in the intact hemiretinae were lower than that of healthy eyes. To our knowledge, however, there are no reports on the retinal vascular integrity of glaucoma eyes in which visual field damage is localized to a single-hemifield. Hence the current study is unique in that diffuse attenuation of vessel density was identified in both peripapillary and macular regions of glaucoma eyes with focal visual field damage confined to a single-hemifield.

Arend et al.[27] examined the effect of asymmetric altitudinal visual field damage on retinal microcirculation obtained by fluorescein angiography in a cohort group of normal tension glaucoma (NTG) eyes. They reported that in hemiretinae with more severe glaucomatous visual field damage the arteriovenous passage (AVP) time is significantly reduced compared to the opposite hemiretinae and also both affected and less affected hemispheres showed increased AVP time compared to healthy eyes. In another study, Hall and associates[28] reported a strong association between decreased diameter of the peripapillary arterioles and visual field loss in the corresponding hemifields of eyes with visual field loss predominantly in one hemifield. The authors suggested that their results could either reflect an ischemic basis for glaucomatous damage or an effect of neural tissue loss leading to vasoconstriction. It is worth mentioning that the inclusion criteria for both studies were having asymmetric visual field damage and the study populations were different from studies investigating perimetrically intact areas of glaucoma eyes with local visual field damage such as the present study.

More recently, Sehi and colleagues[15] used Doppler-OCT to evaluate total retinal blood flow in both affected and unaffected hemiretinae of glaucoma eyes with visual field defects

confined to a single-hemifield. Using a different instrument to assess vascular integrity, their results also showed that total retinal blood flow as well as the mean RNFL and GCC thickness measurements were reduced in the hemiretinae corresponding to the abnormal hemifields compared to the opposite hemiretinae in glaucoma eyes and also these measurements in the unaffected hemiretinae of glaucoma eyes were found to be significantly lower than similar measurements in healthy hemiretinae.

Early studies using OCT-A in glaucoma have documented reduction of vessel density measurements in the overall peripapillary region and its associations with functional measurements.[18, 29] Results of the current study support findings of previous reports; however, in the present study measurements were specifically investigated in both affected and intact hemiretinae of eyes with localized visual field defects confined to a single hemifield. This approach was chosen as it facilitated direct assessment of visual field damage and its corresponding retinal microcirculation. In addition, our findings were also suggestive of more widespread peripapillary and macular vascular damage in the intact hemiretina of glaucoma eyes than detectable by perimetry.

In the present study, it was also observed that the correlation between visual field indices and vessel density in both affected and intact hemiretinae of glaucoma eyes were generally stronger than the relationships between visual field indices and SD-OCT based structural damage. Moreover, as could be expected, associations were stronger in the affected compared to the intact hemifields. In the intact hemifield, all visual field parameters except PD were found to be associated with both structural and vascular measures. One explanation for this finding in the intact hemifield is that eyes with any test locations <1% on the PD plot in the intact hemifield were excluded. Visual field MS and TD could suggest a more widespread loss of vascular and neural tissue occurring in the intact hemiretinae that is associated with the diffuse attenuation of visual function in the intact hemifields. Similarly, Takagi et al.[13] reported an association between SD-OCT macular ganglion cell complex thickness with visual field TD in the intact hemifields of glaucoma eyes and failed to establish an association with visual field PD.

The results of the present study showing stronger associations between visual field measures and OCT-A derived vascular measurements than standard structural measurements are consistent with findings from other OCT-A studies,[17-19, 30] that evaluated relationships between average optic disc and peripapillary vascular measurements with global visual field indices such as MD and PSD.[17-19] More recently Akagi et al.,[22] studied eyes with hemifield visual field defects using OCT-A and reported that peripapillary vessel density in both non-myopic and myopic eyes was reduced at the corresponding location of the visual field defects and was associated with the visual field TD values at their corresponding sides. The current study has further shown that not only the peripapillary microvasculature in the optic nerve head but also microvascular networks in the perifoveal region of the macula is reduced both in the affected and intact hemiretinae of glaucoma eyes. Longitudinal studies are needed to clarify the clinical and pathophysiological relevance of perifoveal reduced vessel density in glaucomatous neuropathy.

In contrast, in a study using Doppler-OCT, a relationship between total retinal blood flow in either the affected or intact hemiretinae and retinal sensitivity in the corresponding hemifields was not established.[15] We speculate that the difference in the results of the present study with the aforementioned study could be partially attributed to the different aspects of the ocular vasculature assessed by different technologies. Doppler-OCT technology is able to quantify retinal blood flow within the large vessels, however flow velocity in the microvasculature is too low to be detected by Doppler shift.[31-33] In contrast, OCT-A measures the presence of blood flow as characterized by moving red blood cells.[17, 25] Moreover, OCT-A technology unlike Doppler is not sensitive to the direction of vasculature in relation to the direction of the emitting beam. Hence OCT-A captures the dynamic motion of flowing blood in all directions in contrast to Doppler that quantifies flow velocity depending on their orientation and angle of the vasculature in relationship to the incident beam. Comparison of validated measures of retinal blood flow such as Doppler-OCT with OCT-A vessel density measurements in longitudinal studies may elucidate the importance of the vascular bed they measure.

We also found a stronger association of the visual function with both peripapillary and macular vessel density compared to structural measurements in the similar regions in the affected hemifields of glaucoma eyes ($p < 0.05$). We speculate that these results could reflect the existence of dysfunctional RGCs with lower metabolic demands, and/ or vascular dropout while these cells have not atrophied yet to be detected via imaging the structural tissue.[34, 35] In other words, characterizing the vasculature by detection of RBCs flowing to meet the metabolic needs of cells could possibly be a surrogate for neural tissue oxygenation and metabolism and may better reflect functional status of the RGCs than the structural measurements alone. Longitudinal studies are needed to determine how retinal vasculature is involved in the pathophysiology of glaucoma and whether OCT-A vascular parameters can provide important information for clinical management of the disease that is not reflected in current structural measurements.

OCT-A is a new imaging modality that enables visualization of ocular vasculature in various retinal layers. Results of the present study suggest that OCT-A is able to detect diffuse reduction of vasculature that exists in glaucoma eyes with localized functional damage. However it should be noted that vascular measurements obtained by this technology only reflect some aspects of flowing blood within the detected vessels and is not an estimate of blood flow or other aspects of ocular circulation. The Angiovue detects vasculature based on amplitude decorrelation, which results from blood flow, but does not directly quantify the flow rate within detected vessels.[36] Therefore, reduced vessel density that we observed could be either the result of capillary dropout or of very slow rates of blood flow within perfused vasculature and results should be interpreted having these two scenarios in mind.

Our study has several limitations. First, due to the cross-sectional design, we could only identify detectable microvascular attenuation and its association with functional measures in glaucoma eyes, and we were not able to establish any cause and effect relationships. Finding attenuated vasculature that is correlated with visual field measures could indicate vascular damage relevant to the pathophysiology of glaucoma, although it cannot distinguish between decreased vessel density caused by structural damage as a consequence of glaucoma and

ischemia, a potential cause of the damage. It is possible that structural damage drives the reduction in vessel density through decreased metabolic demand or alternatively neural tissue loss arises from the attenuated microvasculature and the resulting ischemic damage.[37-39] Longitudinal studies can further clarify these relationships. Second, in using the PD plot in defining a defect, which compares results to a normative database, it is important to remember that this does not preclude possible diffuse functional damage, which is especially common in early glaucoma.[40] As a result, it is important to remember that intact hemifields reported in this study and others do not necessarily have a total absence of true visual field loss (though this is may be hard to detect or quantify due to noisy measurements, aging and/or cataract). Finally, due to the cross-sectional, non-interventional design of the study we were not able to evaluate the potentially confounding impact of ocular hypertensive drops, blood pressure lowering medications and systemic conditions on the vascular measurements. Among glaucoma eyes, moreover, 48 (82.8%) were taking multiple ocular hypertensive drops for a lengthy time. Therefore despite finding no differences in BP, IOP or MOPP measurements, systemic conditions and the use of systemic medications between our study populations we cannot dismiss the effect of these factors on vascular measurements. Hence, exploring the possible effect of ocular and systemic conditions and the use of medications on vascular measurements warrant further investigations.

In conclusion, we have demonstrated that in glaucoma eyes with a single-hemifield defect, vessel density and structural measurements were reduced in the intact hemiretinae in both peripapillary and macular regions compared to hemiretinae of healthy eyes. In addition, the amount of structural damage and vessel density loss in both affected and intact hemiretinae were found to be associated with the extent of perimetric loss in the corresponding hemifields and these associations were generally stronger for vascular measurements compared to structural measurements. OCT-A is a promising technology that is able to detect microvascular dropout in regions without detectable visual field loss and it might further improve our understanding about the role of retinal vasculature in glaucoma. Longitudinal studies are needed to determine the complex topographic and temporal relationship between progressive changes in retinal vasculature, and structural and functional measurements.

Acknowledgments

Supported in part by National Institutes of Health/National Eye Institute grants EY011008 (L.M.Z.), EY14267 (L.M.Z.), EY019869 (L.M.Z.), core grant P30EY022589; an unrestricted grant from Research to Prevent Blindness (New York, NY); grants for participants' glaucoma medications from Alcon, Allergan, Pfizer, Merck, and Santen; a National Health and Medical Research Council (NHMRC) Early Career Fellowship (#1104985; Z.W.).

References

1. Weinreb RN, Khaw PT. Primary open-angle glaucoma. Lancet. 2004; 363(9422):1711–20. [PubMed: 15158634]
2. Flammer J, Orgul S, Costa VP, et al. The impact of ocular blood flow in glaucoma. Prog Retin Eye Res. 2002; 21(4):359–93. [PubMed: 12150988]
3. Weinreb, RN., Harris, A., editors. Ocular Blood Flow in Glaucoma. Amsterdam, The Netherlands: Kugler Publications; 2009.

4. Harris A, Kagemann L, Cioffi GA. Assessment of human ocular hemodynamics. Surv Ophthalmol. 1998; 42(6):509–33. [PubMed: 9635901]
5. Harris A, Chung HS, Ciulla TA, Kagemann L. Progress in measurement of ocular blood flow and relevance to our understanding of glaucoma and age-related macular degeneration. Prog Retin Eye Res. 1999; 18(5):669–87. [PubMed: 10438154]
6. Schuman JS. Measuring Blood Flow: So What? JAMA Ophthalmol. 2015; 133(9):1052–3. [PubMed: 26203625]
7. Harris A, Kagemann L, Ehrlich R, et al. Measuring and interpreting ocular blood flow and metabolism in glaucoma. Can J Ophthalmol. 2008; 43(3):328–36. [PubMed: 18443609]
8. Bagga H, Greenfield DS. Quantitative assessment of structural damage in eyes with localized visual field abnormalities. Am J Ophthalmol. 2004; 137(5):797–805. [PubMed: 15126142]
9. Bagga H, Greenfield DS, Knighton RW. Macular symmetry testing for glaucoma detection. J Glaucoma. 2005; 14(5):358–63. [PubMed: 16148583]
10. Choi J, Cho HS, Lee CH, Kook MS. Scanning laser polarimetry with variable corneal compensation in the area of apparently normal hemifield in eyes with normal-tension glaucoma. Ophthalmology. 2006; 113(11):1954–60. [PubMed: 16935338]
11. Grewal DS, Sehi M, Greenfield DS. Diffuse glaucomatous structural and functional damage in the hemifield without significant pattern loss. Arch Ophthalmol. 2009; 127(11):1442–8. [PubMed: 19901209]
12. Kook MS, Sung K, Kim S, et al. Study of retinal nerve fibre layer thickness in eyes with high tension glaucoma and hemifield defect. Br J Ophthalmol. 2001; 85(10):1167–70. [PubMed: 11567958]
13. Takagi ST, Kita Y, Yagi F, Tomita G. Macular retinal ganglion cell complex damage in the apparently normal visual field of glaucomatous eyes with hemifield defects. J Glaucoma. 2012; 21(5):318–25. [PubMed: 21423034]
14. Na JH, Kook MS, Lee Y, et al. Detection of macular and circumpapillary structural loss in normal hemifield areas of glaucomatous eyes with localized visual field defects using spectral-domain optical coherence tomography. Graefes Arch Clin Exp Ophthalmol. 2012; 250(4):595–602. [PubMed: 22169979]
15. Sehi M, Goharian I, Konduru R, et al. Retinal blood flow in glaucomatous eyes with single-hemifield damage. Ophthalmology. 2014; 121(3):750–8. [PubMed: 24290800]
16. Jia Y, Bailey ST, Hwang TS, et al. Quantitative optical coherence tomography angiography of vascular abnormalities in the living human eye. Proc Natl Acad Sci U S A. 2015; 112(18):E2395–402. [PubMed: 25897021]
17. Jia Y, Morrison JC, Tokayer J, et al. Quantitative OCT angiography of optic nerve head blood flow. Biomed Opt Express. 2012; 3(12):3127–37. [PubMed: 23243564]
18. Liu L, Jia Y, Takusagawa HL, et al. Optical Coherence Tomography Angiography of the Peripapillary Retina in Glaucoma. JAMA Ophthalmol. 2015; 133(9):1045–52. [PubMed: 26203793]
19. Wang X, Jiang C, Ko T, et al. Correlation between optic disc perfusion and glaucomatous severity in patients with open-angle glaucoma: an optical coherence tomography angiography study. Graefes Arch Clin Exp Ophthalmol. 2015; 253(9):1557–64. [PubMed: 26255817]
20. Yu J, Jiang C, Wang X, et al. Macular perfusion in healthy Chinese: an optical coherence tomography angiogram study. Invest Ophthalmol Vis Sci. 2015; 56(5):3212–7. [PubMed: 26024105]
21. Yarmohammadi A, Zangwill LM, Diniz-Filho A, et al. Optical Coherence Tomography Angiography Vessel Density in Healthy, Glaucoma Suspect, and Glaucoma Eyes. Invest Ophthalmol Vis Sci. 2016; 57(9):OCT451–9. [PubMed: 27409505]
22. Akagi T, Iida Y, Nakanishi H, et al. Microvascular Density in Glaucomatous Eyes with Hemifield Visual Field Defects: An Optical Coherence Tomography Angiography Study. Am J Ophthalmol. 2016; 168:237–49. [PubMed: 27296492]
23. Suh MH, Zangwill LM, Manalastas PI, et al. Optical Coherence Tomography Angiography Vessel Density in Glaucomatous Eyes with Focal Lamina Cribrosa Defects. Ophthalmology. 2016; 123(11):2309–17. [PubMed: 27592175]

24. Sample PA, Girkin CA, Zangwill LM, et al. The African Descent and Glaucoma Evaluation Study (ADAGES): design and baseline data. Arch Ophthalmol. 2009; 127(9):1136–45. [PubMed: 19752422]
25. Jia Y, Tan O, Tokayer J, et al. Split-spectrum amplitude-decorrelation angiography with optical coherence tomography. Opt Express. 2012; 20(4):4710–25. [PubMed: 22418228]
26. Spaide RF, Klancnik JM Jr, Cooney MJ. Retinal vascular layers imaged by fluorescein angiography and optical coherence tomography angiography. JAMA Ophthalmol. 2015; 133(1):45–50. [PubMed: 25317632]
27. Arend O, Remky A, Cantor LB, Harris A. Altitudinal visual field asymmetry is coupled with altered retinal circulation in patients with normal pressure glaucoma. Br J Ophthalmol. 2000; 84(9):1008–12. [PubMed: 10966955]
28. Hall JK, Andrews AP, Walker R, Piltz-Seymour JR. Association of retinal vessel caliber and visual field defects in glaucoma. Am J Ophthalmol. 2001; 132(6):855–9. [PubMed: 11730648]
29. Yarmohammadi AZL, Diniz-Filho A, Suh MH, Malastas PI, Fatehee N, Yousefi S, Belghith A, Medeiros FA, Huang D, Weinreb RN. Optical coherence tomography angiography vessel density in healthy, glaucoma suspects, and glaucoma eyes. Invest Ophthalmol Vis Sci. 2016 In press.
30. Yarmohammadi A, Zangwill LM, Diniz-Filho A, et al. Relationship between Optical Coherence Tomography Angiography Vessel Density and Severity of Visual Field Loss in Glaucoma. Ophthalmology. 2016; 123(12):2498–508. [PubMed: 27726964]
31. Chen Z, Milner TE, Srinivas S, et al. Noninvasive imaging of in vivo blood flow velocity using optical Doppler tomography. Opt Lett. 1997; 22(14):1119–21. [PubMed: 18185770]
32. Leitgeb R, Schmetterer L, Drexler W, et al. Real-time assessment of retinal blood flow with ultrafast acquisition by color Doppler Fourier domain optical coherence tomography. Opt Express. 2003; 11(23):3116–21. [PubMed: 19471434]
33. Wang Y, Bower BA, Izatt JA, et al. Retinal blood flow measurement by circumpapillary Fourier domain Doppler optical coherence tomography. J Biomed Opt. 2008; 13(6):064003. [PubMed: 19123650]
34. Cherecheanu AP, Garhofer G, Schmidl D, et al. Ocular perfusion pressure and ocular blood flow in glaucoma. Curr Opin Pharmacol. 2013; 13(1):36–42. [PubMed: 23009741]
35. Chauhan BC, Stevens KT, Levesque JM, et al. Longitudinal in vivo imaging of retinal ganglion cells and retinal thickness changes following optic nerve injury in mice. PLoS One. 2012; 7(6):e40352. [PubMed: 22768284]
36. Tokayer J, Jia Y, Dhalla AH, Huang D. Blood flow velocity quantification using split-spectrum amplitude-decorrelation angiography with optical coherence tomography. Biomed Opt Express. 2013; 4(10):1909–24. [PubMed: 24156053]
37. Caprioli J, Coleman AL, Blood Flow in Glaucoma D. Blood pressure, perfusion pressure, and glaucoma. Am J Ophthalmol. 2010; 149(5):704–12. [PubMed: 20399924]
38. Hwang JC, Konduru R, Zhang X, et al. Relationship among visual field, blood flow, and neural structure measurements in glaucoma. Invest Ophthalmol Vis Sci. 2012; 53(6):3020–6. [PubMed: 22447865]
39. Yu PK, Balaratnasingam C, Xu J, et al. Label-Free Density Measurements of Radial Peripapillary Capillaries in the Human Retina. PLoS One. 2015; 10(8):e0135151. [PubMed: 26252395]
40. Henson DB, Artes PH, Chauhan BC. Diffuse loss of sensitivity in early glaucoma. Invest Ophthalmol Vis Sci. 1999; 40(13):3147–51. [PubMed: 10586936]

Abbreviations and Acronyms

-A	angiography
CCT	central corneal thickness
CI	confidence interval
cpVD	circumpapillary vessel density

dB	decibels
DIGS	Diagnostic Innovations in Glaucoma Study
GCC	ganglion cell thickness
IOP	intraocular pressure
MD	mean deviation
MS	mean sensitivity
μm	micrometers
OCT	optical coherence tomography
PD	pattern deviation
pfVD	perifoveal vessel density
POAG	primary open-angle glaucoma
PSD	pattern standard deviation
RGC	retinal ganglion cell
RNFL	retinal nerve fiber layer
SAP	standard automated perimetry
SD	spectral domain
SSADA	split spectrum amplitude decorrelation angiography
TD	total deviation

Precis / Highlights

OCT angiography is able to detect microvascular dropouts in peripapillary and macular regions without detectable visual field loss, and it may enhance our understanding of the role of retinal vasculature in glaucoma.

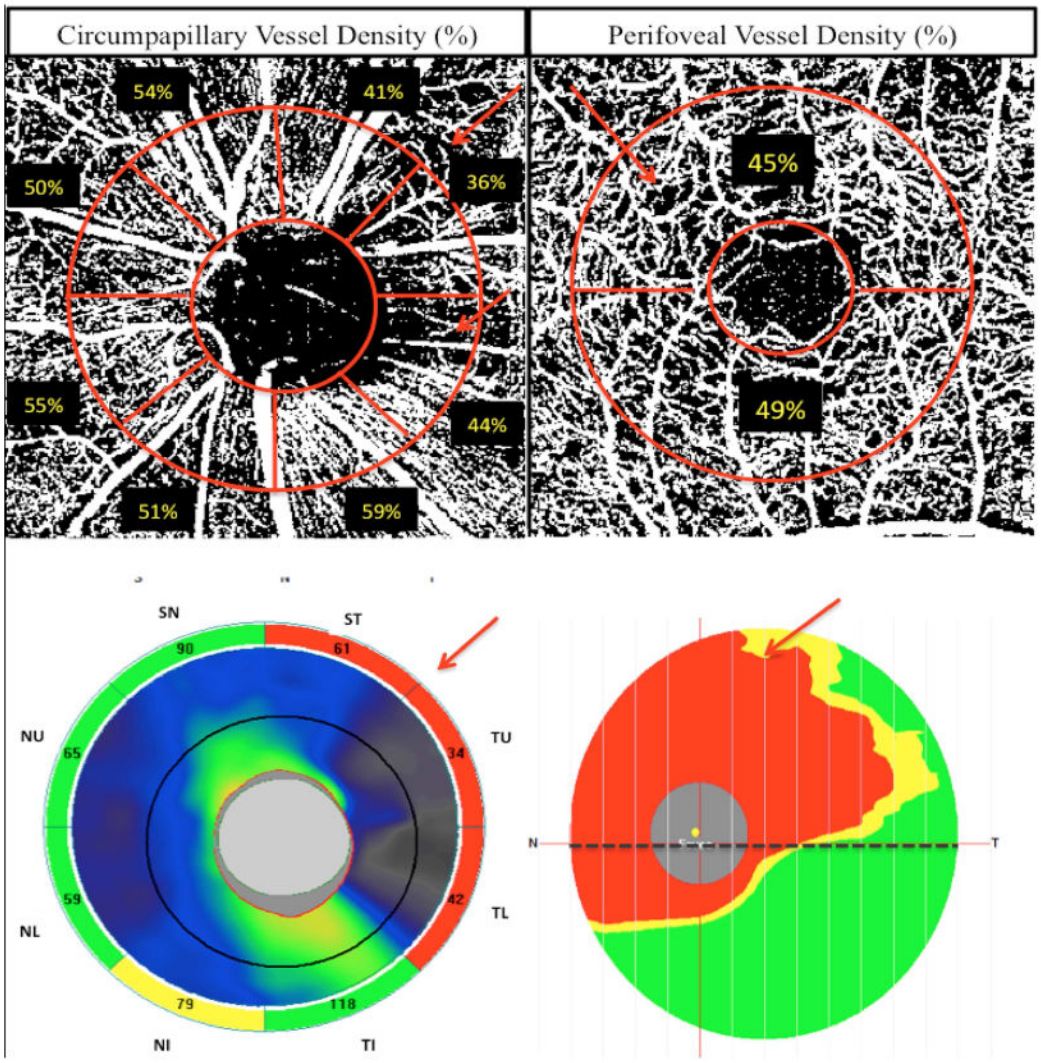

Figure 1.

Top row: Vessel density map of the peripapillary retinal nerve fiber layer with circumpapillary (cpVD) measurement region defined (left) and macular superficial layer with perifoveal (pfVD) measurement region defined (right). Bottom row: spectral domain optical coherence tomography (SD-OCT) optic nerve head (ONH) thickness map (left) and macular ganglion cell complex (mGCC) thickness map (right).

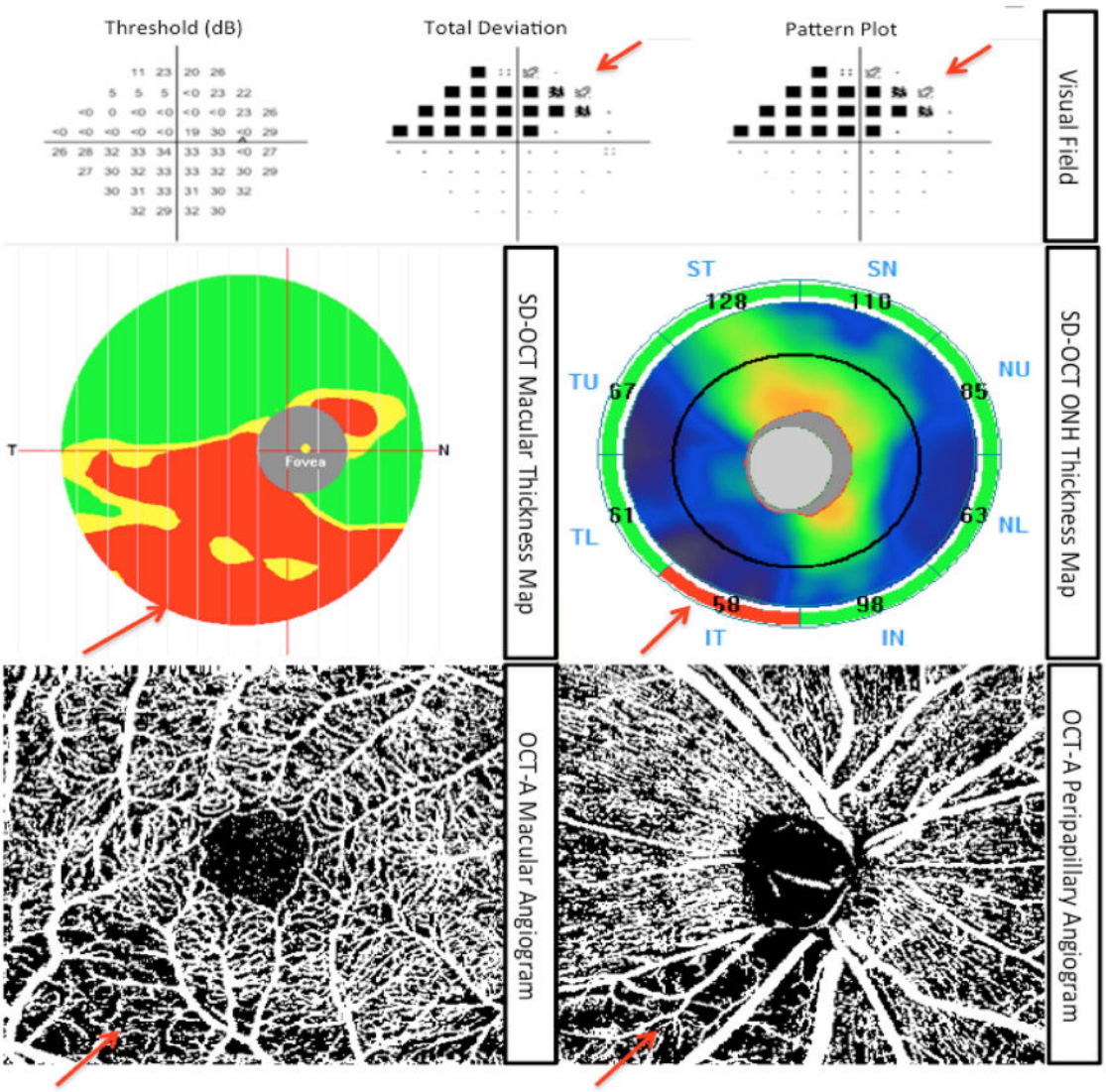

Figure 2.

A representative glaucoma eye with superior visual field defect: Top row: standard automated perimetry (SAP) results showing superior visual field. Middle row: macular ganglion cell complex (mGCC) thickness map (left) and optic nerve head (ONH) thickness map (right) representing mGCC and circumpapillary retinal nerve fiber layer (cpRNFL) loss corresponding to the visual field defect. Bottom line: Vessel density map of the peripapillary retinal nerve fiber layer (right) and macular superficial layer (left) illustrating reduced vasculature that spatially correlates with the location of structural loss and visual field defect.

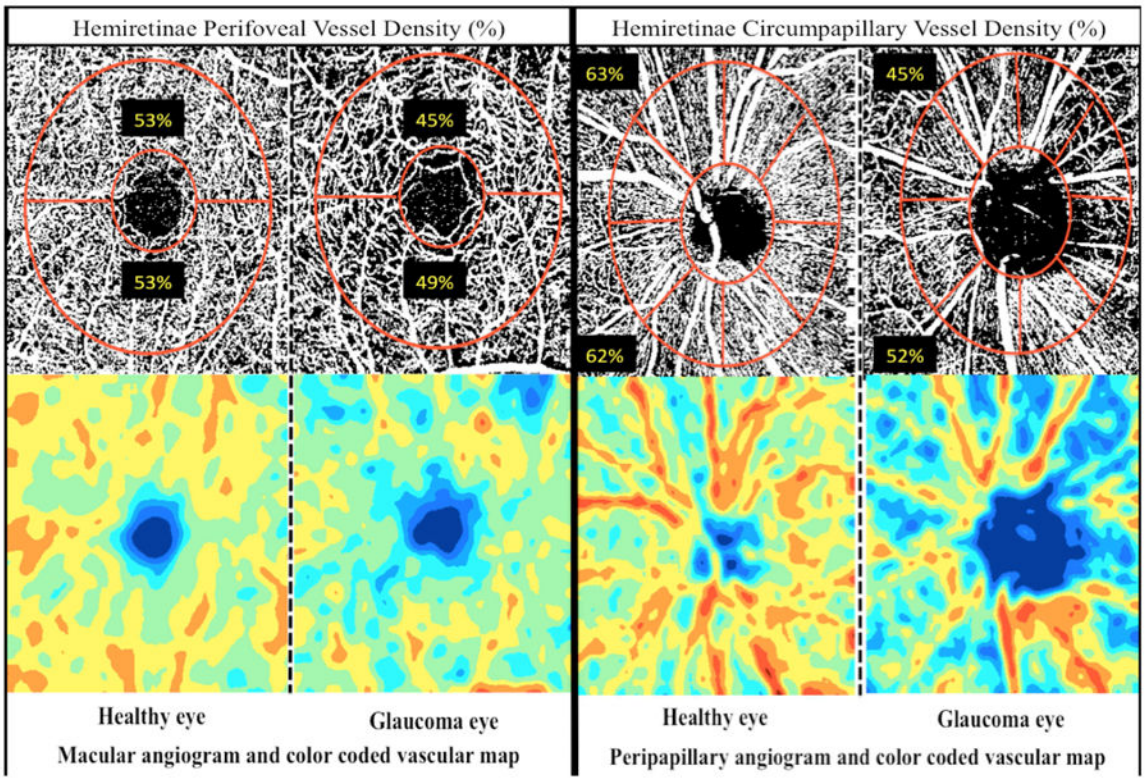

Figure 3.

Top row: Vessel density map of the macular superficial layer (left) and peripapillary retinal nerve fiber layer (right) showing denser microvascular networks in healthy eyes in both regions. Bottom row: Area vessel density color-coded map of the macular superficial layer (left) and peripapillary retinal nerve fiber layer (right), in which the orange color indicates a vessel density of greater than 50% perfused vessels, dark blue indicates no perfused vessels detected, and intermediate vessel density values vary from yellow to green.

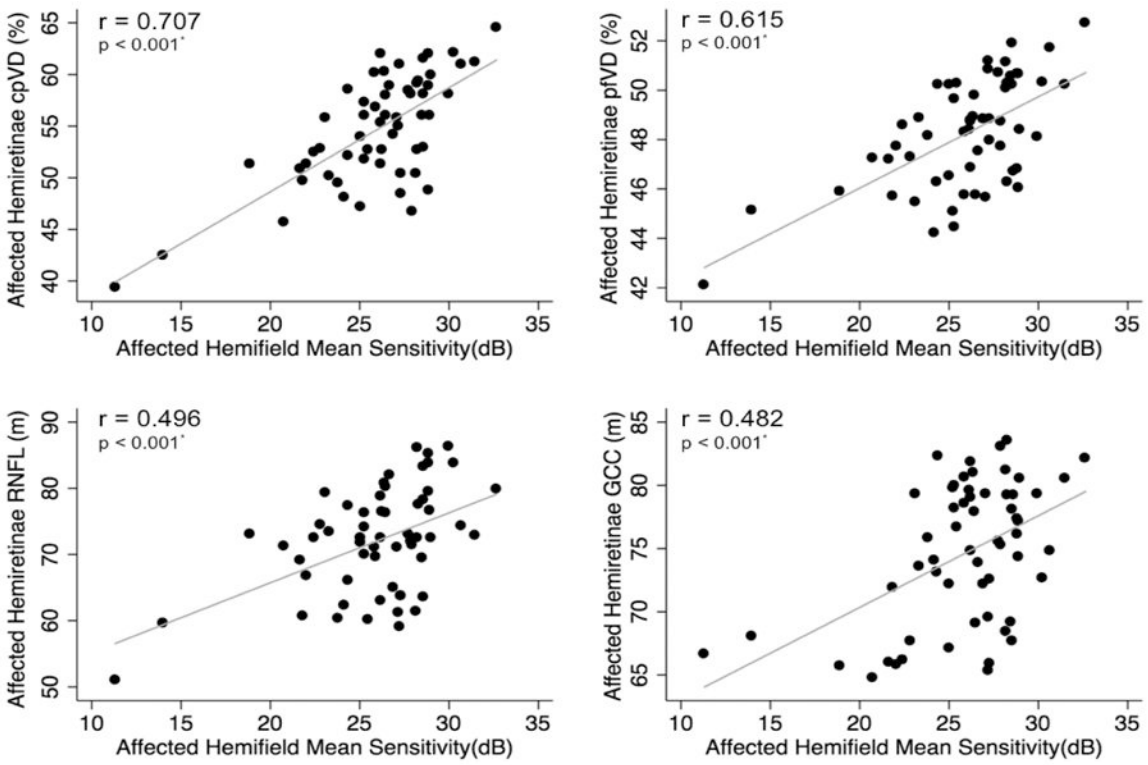

Figure 4.

Scatterplots illustrating the linear (grey line) associations between standard automated perimetry (SAP) mean sensitivity in the affected hemifields and optical coherence tomography angiography (OCT-A) circumpapillary vessel density (cpVD), perifoveal vessel density (pfVD), spectral domain optical coherence tomography (SD-OCT) retinal nerve fiber layer (RNFL) and ganglion cell complex (GCC) thickness measurements in the corresponding hemiretinae of glaucoma eyes. r: correlation coefficient from the fitted linear regression model.

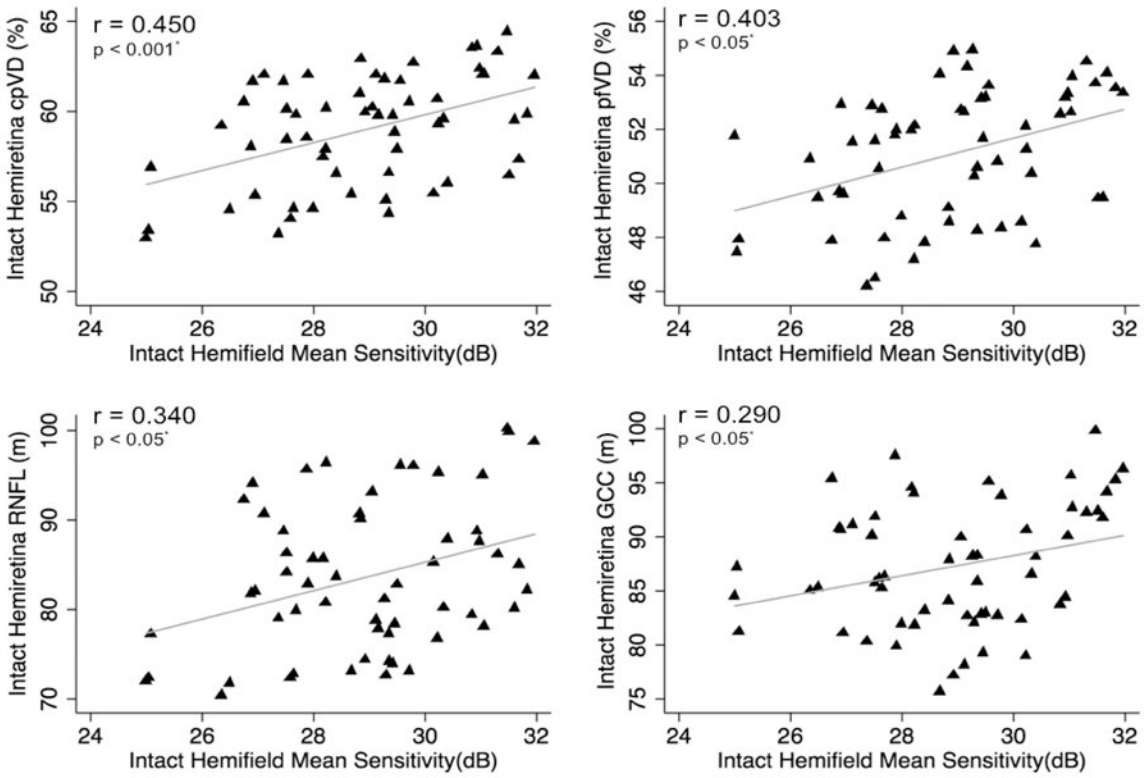

Figure 5.

Scatterplots illustrating the linear (grey line) associations between standard automated perimetry (SAP) mean sensitivity in the perimetrically intact hemifields and optical coherence tomography angiography (OCT-A) circumpapillary vessel density (cpVD), perifoveal vessel density (pfVD), spectral domain (SD) OCT retinal nerve fiber layer (RNFL) and ganglion cell complex (GCC) thickness measurements in the corresponding hemiretinae of glaucoma eyes. r: correlation coefficient from the fitted linear regression model.

Table 1
Demographics and Ocular Characteristics of the Study Population

Variables	Healthy eyes (28 eyes of 28 patients)	Glaucoma eyes (58 eyes of 58 patients)	P-value
Age (years)	69.91 ± 9.28	71.37 ± 9.75	0.190‡
Gender (male/female)	8/20	24/34	0.250†
Ethnicity (AD/ED)	12/16	10/48	0.011†
VF defect location (Sup/Inf), n	NA	26/32	
SE (D)	-0.17 ± 1.41	-0.89 ± 2.16	0.217*
CCT (μm)	540.11± 42.91	534.66 ± 40.06	0.576‡
IOP (mmHg)	15.71 ± 3.31	14.11 ± 4.74	0.076‡
Hypertension, n (%)	13 (46.4 %)	28 (48.3 %)	0.872†
Diabetes, n (%)	5 (17.9 %)	5 (8.6 %)	0.211†
Cardiovascular disease, n (%)	4 (14.3 %)	12 (20.7 %)	0.475†
Hypertension medication, n (%)	14 (50.0%)	30 (51.7%)	0.881†
Diabetic medication, n (%)	4 (14.3%)	5 (8.6%)	0.421†
SBP (mmHg)	132.32 ± 19.09	127.39 ±17.39	0.110*
DBP (mmHg)	82.23 ± 12.17	78.67 ± 11.45	0.209*
MOPP (mmHg)	52.01 ± 9.25	49.16 ± 9.19	0.186‡
SAP mean deviation (dB)	-0.10 ± 1.12	-3.68 ± 3.38	<0.001*
SAP pattern standard deviation (dB)	1.66 ± 0.43	5.78 ± 4.04	<0.001*
Disc area (mm^2)	1.98 ± 0.45	1.98 ± 0.45	0.661‡
Rim area (mm^2)	1.31 ± 0.27	0.83 ± 0.37	<0.001‡
Average cpVD (%)	62.5 ± 3.6	57.0± 4.7	<0.001‡
Average pfVD (%)	53.9 ± 2.4	49.7 ± 3.1	<0.001‡
Average cpRNFL (μm)	94.9 ± 8.4	77.7 ± 9.2	<0.001‡
Average mGCC (μm)	92.3 ± 6.7	82.2 ± 9.0	<0.001‡

Values are shown in mean ± standard deviation

*The comparison was performed by using Mann-Whitney test.

†The comparison was performed by using Chi-squared test.

‡The comparison was performed by using independent samples t-test

AD: African descent; ED: European descent; VF: visual field; SE: spherical equivalent; CCT: central corneal thickness; IOP: intraocular pressure; SBP: systolic blood pressure; DBP: diastolic blood pressure; MOPP: mean ocular perfusion pressure; SAP: standard automated perimetry; cpVD: circumpapillary vessel density; pfVD: perifoveal vessel density; cpRNFL: circumpapillary retinal nerve fiber layer; mGCC: macular ganglion cell complex

Table 2

Visual Field, Structural and Vascular Measurements Corresponding to the Affected and Intact Hemifields

Variables	Healthy eyes (n = 28)	Glaucoma eyes (n = 58)		p-value^{A}	p-value^{B}	p-value^{C}
		Intact hemifield	Affected hemifield			
SAP mean sensitivity (dB)	30.0 ± 1.7	29.0 ± 1.8	26.0 ± 3.7	0.089‡	**<0.001***	**<0.001**§
SAP total deviation (dB)	0.1 ± 1.4	-0.1 ± 1.4	-6.7 ± 6.4	0.076‡	**<0.001***	**<0.001**§
SAP pattern deviation (dB)	-1.3 ± **0.3**	-1.3 ± **0.3**	-7.3 ± 6.1	0.189‡	**<0.001***	**<0.001**§
Circumpapillary vessel density (%)	62.4 ± **2.9**	59.0 ± 3.1	54.7 ± 5.3	**<0.001**‡	**<0.001**‡	**<0.001**†
Perifoveal vessel density (%)	53.8 ± 2.1	51.1 ± **2.4**	48.3 ± 4.2	**<0.001**‡	**<0.001**‡	**<0.001**†
Retinal nerve fiber layer thickness (μm)	95.0 ± **8.2**	83.6 ± **9.3**	72.1 ±10.9	**<0.001**‡	**<0.001***	**<0.001**§
Ganglion cell complex thickness (μm)	92.4 ± 5.1	87.3 ± 5.8	74.7 ± 7.8	**0.002**‡	**<0.001***	**<0.001**§

Values are shown in mean ± standard deviation

^{A}Comparison between intact hemifield of glaucoma eyes and healthy eyes

^{B}Comparison between affected hemifield of glaucoma eyes and healthy eyes

^{C}Comparison between affected and intact hemifield of glaucoma eyes

‡The Comparison was performed by using independent samples *t*-test

†The Comparison was performed by using paired *t*-test

*The Comparison was performed by using Mann-Whitney U test.

§The Comparison was performed by using Wilcoxon signed-rank test

SAP: standard automated perimetry; dB: decibel; μm: micrometer

Table 3

Associations Between Hemispheric Vascular and Structural Measurements with SAP Functional Measurements in the Corresponding Hemifields

Variables	Intact hemifield and corresponding hemiretinae								Affected hemifield and corresponding hemiretinae							
	cpVD (%)		pfVD (%)		cpRNFL (μm)		mGCC (μm)		cpVD (%)		pfVD (%)		cpRNFL (μm)		mGCC (μm)	
	r	p-value	r	p-value	r	p-value	r	p-value	r	p-value	r	p-value	r	p-value	r	p-value
SAP MS (dB)	0.450	<0.001*	0.403	0.002*	0.340	0.009*	0.290	0.027*	0.707	<0.001*	0.615	<0.001*	0.496	<0.001*	0.482	<0.001*
SAP MS (1/L)	0.418	0.001*	0.400	0.002*	0.335	0.010*	0.329	0.006*	0.605	<0.001*	0.562	<0.001*	0.410	<0.001*	0.395	<0.001*
SAP TD (dB)	0.312	0.010*	0.296	0.036*	0.266	0.043*	0.245	0.045*	0.526	<0.001*	0.517	<0.001*	0.385	<0.001*	0.368	<0.001*
SAP PD (dB)	0.031	0.817	0.019	0.884	0.078	0.560	0.050	0.708	0.471	<0.001*	0.475	<0.001*	0.373	<0.001*	0.310	<0.001*

cpVD: circumpapillary vessel density; pfVD: perifoveal vessel density; cpRNFL: circumpapillary retinal nerve fiber layer; μm: micrometer; mGCC: macular ganglion cell complex; SAP: standard automated perimetry; MS: mean sensitivity; dB: decibel; L: Lambert; TD: total deviation; PD: pattern deviation